

# Computer-generated space-variant polarization elements with subwavelength metal stripes

Ze'ev Bomzon, Vladimir Kleiner, and Erez Hasman

Optical Engineering Laboratory, Faculty of Mechanical Engineering, Technion-Israel Institute of Technology, Haifa 32000, Israel

Received July 28, 2000

A novel method of performing two-dimensional space-variant polarization operations is presented. The method is based on determining the local direction and period of subwavelength metal-stripe gratings by use of vectorial optics to obtain any desired continuous polarization change. We demonstrate our approach with specific computer-generated space-variant polarization elements for laser radiation at  $10.6 \mu\text{m}$ . The polarization properties are verified with complete space-variant polarization analysis and measurement.

© 2001 Optical Society of America

OCIS codes: 260.5430, 260.2130, 050.1950, 350.3950, 050.2770.

Subwavelength metal wire gratings are usually used as polarizers. When the period of the grating is much smaller than the incident wavelength, only light that is polarized perpendicular to the stripes is transmitted through the grating. Metal-stripe gratings are usually linear uniform gratings, which form homogeneous space-invariant polarizers.<sup>1,2</sup> Sometimes, however, different polarization is required at each location. Such nonuniform space-variant polarization is useful for polarization coding of data in optical communication, optical computers<sup>3</sup> and neural networks, optical encryption,<sup>4</sup> tight focusing,<sup>5</sup> imaging polarimetry,<sup>6</sup> and particle trapping and acceleration.<sup>7</sup>

In this Letter we present a method of designing, analyzing, and realizing computer-generated space-variant metal-stripe polarization elements. We show that by determination of the local direction as well as the period of the metal grating by use of vectorial-optics calculations the desired polarization change can be obtained. Moreover, our method ensures that the metal-stripe gratings are continuous over the entire aperture of the two-dimensional elements; therefore any diffraction arising from polarization discontinuity is completely suppressed.<sup>4</sup> We demonstrate our method with a specific space-variant polarization element.

Figure 1 illustrates the geometry of the polarization ellipse of light transmitted through a subwavelength grating. The grating vector, which is perpendicular to the stripes, is

$$\mathbf{K}_g = K_0 \cos(\beta)\hat{x} + K_0 \sin(\beta)\hat{y}, \quad (1)$$

where  $\hat{x}$  and  $\hat{y}$  are unit vectors in the  $x$  and  $y$  directions, respectively,  $K_0 = 2\pi/\Lambda$  is the spatial frequency of a grating of period  $\Lambda$ , and  $\beta$  is the direction of the vector. The transmitted field is, in general, elliptically polarized and can be defined by the azimuthal angle,  $\psi$ , which is the angle between the  $x$  axis and the large axis of the ellipse, and the ellipticity,  $\chi$ , where  $\tan(\chi) = b/a$  is the ratio between the two axes of the ellipse.<sup>8</sup> We define an additional angle  $\Delta\psi$  as the angle between the large axis of the ellipse and the grating vector.

To investigate the dependence of  $\chi$  and  $\Delta\psi$  on the period of the grating we calculated and measured the ellipticity and azimuthal angle for metal-stripe gratings with various periods. We chose the direction of the grating vector so that  $\psi$  and  $\Delta\psi$  coincided. For this purpose was fabricated a chirped grating with a local period that varied from 2 to  $5 \mu\text{m}$  along 7.5 mm, with a width of 5 mm and duty cycle of 0.5. First a chrome mask of the grating was fabricated by use of high-resolution laser lithography, and then the grating was realized on a  $500\text{-}\mu\text{m}$ -thick semi-insulating GaAs wafer by use of a lift-off technique. The metal stripes consisted of a 10-nm layer of Ti, coated by 60 nm of Au. An antireflection coating was applied to the back side of the wafer.

We illuminated the gratings with circularly polarized light at a wavelength of  $10.6 \mu\text{m}$  from a  $\text{CO}_2$  laser and made four measurements of the transmitted intensity. The first three measurements were made after the light was passed through a polarizer that was oriented horizontally, diagonally ( $45^\circ$ ), or vertically. The fourth measurement involved passing the light through a quarter-wave plate with its fast axis at  $0^\circ$  and then through a polarizer at  $45^\circ$ . We computed the intensity measurements by imaging the grating through a lens onto a Spiricon PyrocamI pyroelectric camera. From these four measurements the

Figure 1 illustrates the geometry of the polarization ellipse of light transmitted through a subwavelength grating. The grating vector, which is perpendicular to the stripes, is

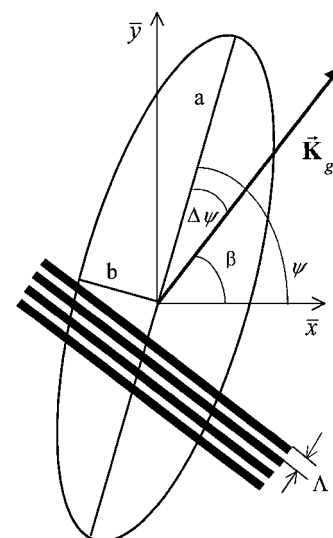


Fig. 1. Geometrical parameters of the polarization ellipse of light transmitted through a subwavelength grating.

Stokes parameters ( $S_0$ – $S_3$ ) could be calculated<sup>8,9</sup> for each point of the grating, and the ellipticity and azimuthal angle could be calculated as  $\tan(2\psi) = S_2/S_1$  and  $\sin(2\chi) = S_3/S_0$ .

The theoretical results were obtained by calculation of the transmitted vector fields by use of rigorous coupled-wave analysis.<sup>10</sup> We then calculated the coherence matrix<sup>9</sup> for the transmitted field, from which the Stokes parameters were derived. Figure 2 shows the measured and the calculated results for the azimuthal angle and the ellipticity of the light transmitted through the chirped grating as a function of the local period. There is good agreement between the measurement and the predicted results. In the region in which the period is much smaller than the incident wavelength,  $\Delta\psi$  and  $\tan(\chi)$  are close to zero, and the transmitted beam is linearly polarized parallel to the grating vector. However, as the period becomes larger, the azimuthal angle and ellipticity increase. When the period approaches  $\lambda/n$ , where  $\lambda$  is the wavelength and  $n$  is the refractive index of the substrate (3.27 for GaAs), we observe a sharp increase in azimuthal angle and in ellipticity. This result seems to be connected to the Wood anomaly.<sup>1</sup>

We conclude that, for incident circularly polarized light,  $\Delta\psi$  varies with the period. Therefore, if we wish to design a grating for which the desired azimuthal angle is  $\psi_{\text{desired}}$ , then the direction of the grating must be such that

$$\beta = \psi_{\text{desired}} - \Delta\psi(K_0) \quad (2)$$

depends on the period of the grating.

Now let us assume that  $\psi_{\text{desired}}$  is space varying. The grating vector is then described as

$$\begin{aligned} \mathbf{K}_g = & K_0(x, y)\cos[\beta(x, y, K_0)]\hat{x} \\ & + K_0(x, y)\sin[\beta(x, y, K_0)]\hat{y}. \end{aligned} \quad (3)$$

For the grating described by Eq. (3) to be physically realizable in a continuous way,  $\mathbf{K}_g$  should be a conserving vector, i.e.,  $\nabla \times \mathbf{K}_g = 0$ , which results in

$$\begin{aligned} & \frac{\partial K_0}{\partial y} \cos(\beta) - K_0 \sin(\beta) \left( \frac{\partial \psi_{\text{desired}}}{\partial y} - \frac{\partial \Delta\psi}{\partial K_0} \frac{\partial K_0}{\partial y} \right) \\ = & \frac{\partial K_0}{\partial x} \sin(\beta) + K_0 \cos(\beta) \left( \frac{\partial \psi_{\text{desired}}}{\partial x} - \frac{\partial \Delta\psi}{\partial K_0} \frac{\partial K_0}{\partial x} \right), \end{aligned} \quad (4)$$

yielding  $\mathbf{K}_g$ . The grating function  $\phi(x, y)$  is then found by integration of  $\mathbf{K}_g$  along any arbitrary path in the  $x$ - $y$  plane so that  $\nabla\phi = \mathbf{K}_g$ .

We applied this method to the design of a space-variant polarization element that permits the transformation of circularly polarized light into a wave whose direction of polarization is a linear function of the  $x$  coordinate,

$$\psi_{\text{desired}} = ax + \psi_0, \quad (5)$$

where  $\psi_0$  is the desired azimuthal angle at  $x = 0$  and  $a$  is a constant.

We can solve Eq. (4) analytically under the zero-order approximation that  $\Delta\psi[K_0(x, y)] = \psi_1$ , where  $\psi_1$  is a constant, to obtain

$$K_0(x, y) = \frac{2\pi}{\Lambda_0} \exp(ay), \quad (6)$$

where  $\Lambda_0$  is the grating period at  $x = 0$ .

Finally, from Eqs. (3), (5), and (6) the grating function is found to be

$$\phi(x, y) = \frac{2\pi}{a\Lambda_0} \sin(ax + \psi_0 - \psi_1)\exp(ay). \quad (7)$$

We designed and realized a Lee-type binary grating described by Eq. (7). Figure 3 shows the magnified geometry of the computer-generated element. We realized an element for  $\Lambda_0 = 2 \mu\text{m}$  and  $a = -18^\circ/\text{mm}$ . The dimensions of the element were  $5 \text{ mm} \times 1 \text{ mm}$ , so  $-90^\circ < \beta < 0^\circ$ ,  $2 \mu\text{m} < \Lambda < 2.8 \mu\text{m}$ , and  $\psi_0 = \psi_1 = 15^\circ$ , which is  $\Delta\psi$  at  $2 \mu\text{m}$ , corresponding to Fig. 2(a). The element was fabricated as a metal-stripe grating with a duty cycle of 0.5 on a  $500\text{-}\mu\text{m}$ -thick GaAs wafer with an antireflection coating on the back side. The metal stripes consisted of an adhesion layer of 10-nm Ti and a layer of 60-nm Au. The fabrication technique was the same as that used for fabrication of the chirped grating.

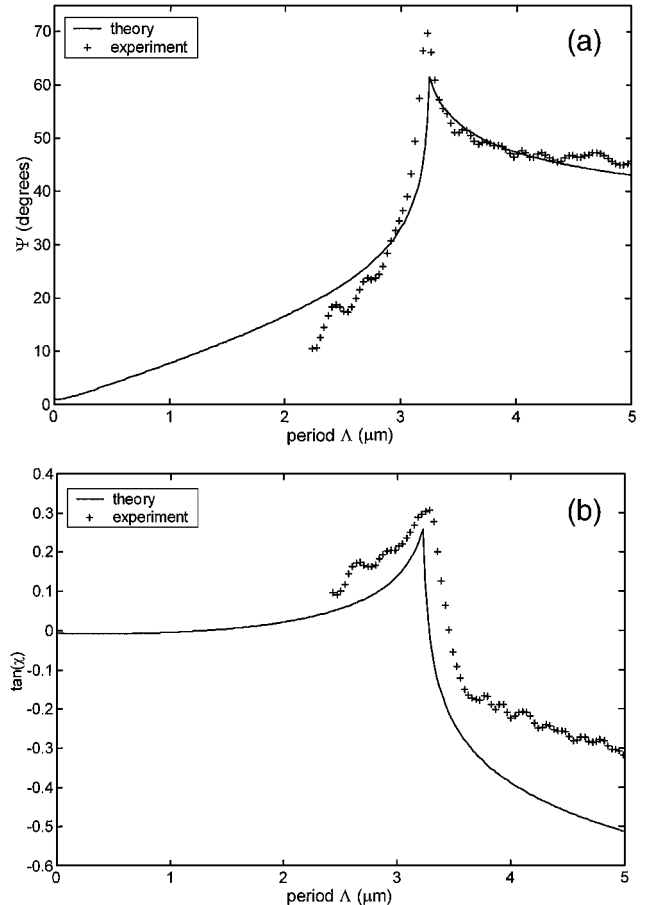


Fig. 2. Measured and calculated results for (a) the azimuthal angle,  $\psi$ , and (b) the ellipticity,  $\tan(\chi)$ , of light transmitted through the chirped grating as a function of the local period.

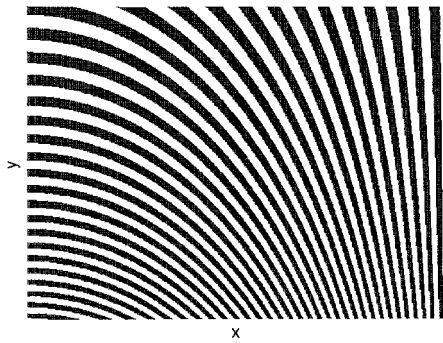


Fig. 3. Magnified illustration of the computer-generated space-variant polarization-element geometry.

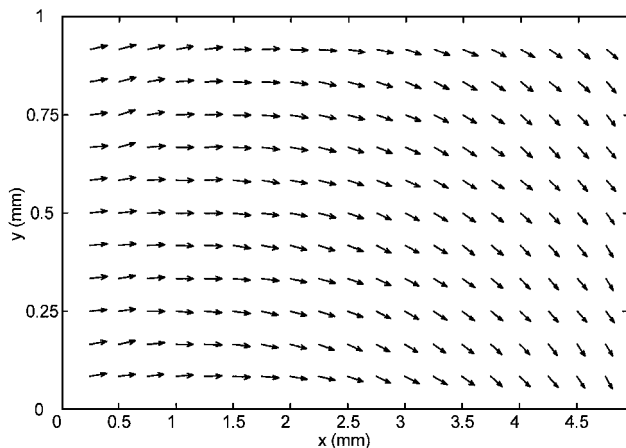


Fig. 4. Experimental measurement of the two-dimensional space-variant polarization orientations. The arrows indicate the direction of the large axis of the local polarization ellipse.

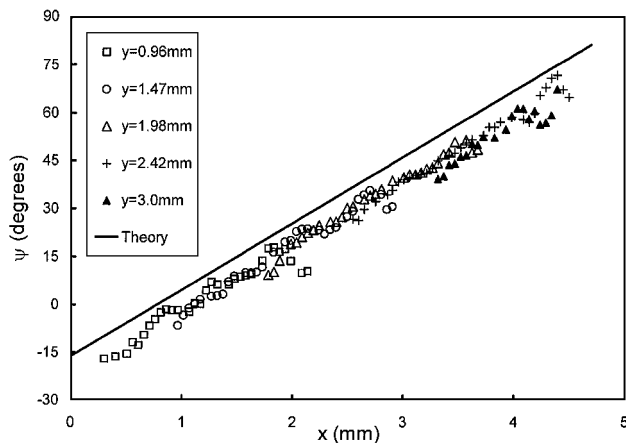


Fig. 5. Measured and calculated azimuthal angles, as a function of  $x$  locations of various  $y$  coordinates, of the space-variant polarization element when it was rotated  $30^\circ$ .

Figure 4 shows experimental measurements of the azimuthal angle for light transmitted through the element when it was illuminated with circularly polarized light. The arrows indicate the direction of the large axis of the local polarization ellipse. The experimental results show that for a constant  $y$  the azimuthal

angle varies linearly as a function of  $x$  over a range of  $90^\circ$ . However, the measurements also show a variation in the  $y$  direction of approximately  $10^\circ$ , which is expected as a result of the variation in period, as seen from the chirped grating. The average measured ellipticity over the entire aperture is  $6^\circ$ . We can decrease the variation of the azimuthal angle along the  $y$  axis by a higher-order approximation of  $\Delta\psi$ . For instance, for the approximation that  $\Delta\psi = \psi_1 + b/K_0$ , we found an approximate solution that is equivalent to a rotation of the element by  $30^\circ$ .

Figure 5 shows the measured and the calculated variations of the azimuthal angle along the  $x$  axis for such an improved configuration. The calculation is based on Jones calculus by use of rigorous coupled-wave analysis. We represented the element as a space-varying Jones matrix, defined by the local period and the orientation of the grating. Figure 5 shows a linear variation of the azimuthal angle along the  $x$  axis and very little variation in the  $y$  direction, with good agreement between experiment and theory. The theoretical result revealed an average deviation of the azimuthal angle from a linear curve of  $0.3^\circ$ , and for the experimental results this deviation was  $3.2^\circ$ , taking into account an average ellipticity of  $6^\circ$ , which gives an overall polarization purity (percentage of power that is polarized in the desired direction) of 98.6%.

To conclude, we have demonstrated a novel approach to the design of high-quality space-variant polarization elements as well as a full space-variant polarization analysis and measurement. Note that it is advantageous to use substrates with lower refractive indices, such as ZnSe, as this extends the range of periods before the Wood anomaly becomes a factor. This approach permits the design of more-efficient elements with a larger range of periods.

This research was supported by the Israel Ministry of Defense. E. Hasman's e-mail address is mehasman@tx.technion.ac.il.

## References

1. M. Honkanen, V. Kettonen, M. Kuittinen, J. Lautanen, J. Turunen, B. Schnabel, and F. Wyrowski, *Appl. Phys. B* **68**, 81 (1999).
2. S. Astilean, Ph. Lalanne, and M. Palamaru, *Opt. Commun.* **175**, 265 (2000).
3. N. Davidson, A. A. Friesem, and E. Hasman, *Appl. Opt.* **31**, 1810 (1992).
4. U. D. Zeitner, B. Schnabel, E-B. Kley, and F. Wyrowski, *Appl. Opt.* **38**, 2177 (1999).
5. S. Quabis, R. Dorn, M. Eberler, O. Glöckl, and G. Leuchs, *Opt. Commun.* **179**, 1 (2000).
6. G. P. Nordin, J. T. Meier, P. C. Deguzman, and M. W. Jones, *J. Opt. Soc. Am. A* **16**, 1168 (1999).
7. Y. Liu, D. Cline, and P. He, *Nucl. Instrum. Methods Phys. Res. A* **424**, 296 (1999).
8. E. Collet, *Polarized Light* (Marcel Dekker, New York, 1993).
9. T. Carozzi, R. Karlsson, and J. Bergman, *Phys. Rev. E* **61**, 2024 (2000).
10. M. G. Moharam and T. K. Gaylord, *J. Opt. Soc. Am. A* **3**, 1780 (1986).